Chronic Inflammation-Induced Senescence Impairs Immunomodulatory Properties of Synovial Fluid Mesenchymal Stem Cells in Rheumatoid Arthritis

Hyeon-Jeong Lee
GNU College of Veterinary Medicine: Gyeongsang National University College of Veterinary Medicine
Won-Jae Lee
Kyungpook National University College of Veterinary Medicine
Sun-Chul Hwang
Gyeongsang National University
Yong-Ho Choi
Gyeongsang National University
Saetbyul Kim
Gyeongsang National University
Eunyeong Bok
Gyeongsang National University
Sangyeob Lee
Gyeongsang National University
Seung-Joon Kim
Kyungpook National University
Hyun-Ok Kim
Gyeongsang National University
Sun-A Ock
Rural Development Administration
Hae Sook Noh
Gyeongsang National University
Gyu-Jin Rho
Gyeongsang National University
Sang-Il Lee
Gyeongsang National University
Sung-Lim Lee (✉ sllee@gnu.ac.kr)
Gyeongsang National University College of Veterinary Medicine https://orcid.org/0000-0002-1055-8097

Research

Keywords: mesenchymal stem cell derived from patient, rheumatoid arthritis, duration of inflammatory disease, immunomodulation, cellular senescence

Posted Date: February 1st, 2021

DOI: https://doi.org/10.21203/rs.3.rs-162096/v1

Abstract

Background

Although immunomodulation properties of mesenchymal stem cells (MSCs) has been highlighted as a new therapy for autoimmune diseases, including rheumatoid arthritis (RA), the alteration of disease-specific characteristics of MSCs derived from elderly RA patients are not well understood.

Methods

We established the MSCs derived from synovial fluid (SF) from age-matched early (average duration of disease: 1.7 years) and long-standing (average duration of disease: 13.8 years) RA patients (E-/L-SF-MSCs) and then comparatively analyzed the characteristics of MSCs such as stemness, proliferation, cellular senescence, *in vitro* differentiation and *in vivo* immunomodulation properties.

Results

The presence of MSC populations in the SF from RA patients was identified and we found that L-SF-MSCs exhibited impaired proliferation, intensified cellular senescence, reduced immunomodulation properties and attenuation of anti-arthritic capacity in an RA animal model than E-SF-MSCs. In particular, E-SF-MSCs demonstrated cellular senescence progression and attenuation of immunomodulation properties at similar levels to that of L-SF-MSCs in an RA joint mimicking milieu due to hypoxia and pro-inflammatory cytokine exposure. Due to long-term exposure to the chronic inflammation milieu, the progression of cellular senescence, attenuation of immunomodulation properties and loss of anti-arthritic potentials are more often identified in SF-MSCs of long-standing RA than early RA.

Conclusion

We conclude that a chronic RA inflammation milieu affected the potential of MSCs; therefore, this work addresses the importance of understanding MSC characteristics during disease states prior to their application in patients.

Background

The onset of rheumatoid arthritis (RA) is associated with loss of the systemic immunological self-tolerance, which results in the activation of autoreactive immune cells against collagen-rich joint regions and symptoms mainly characterized as chronic, destructive inflammation in the joints [1, 2]. As an autoimmune disease, there are limited curative options for RA that immunomodulate and regenerate articular cartilage or subchondral bone in the damaged joints. Mesenchymal stem cells (MSCs) provide notable inhibition of the immune response and are regarded as a potential candidate for various inflammatory autoimmune disease treatment including RA [3]. Once MSCs are exposed to pro-inflammatory cytokines under an inflammation milieu, they are activated and inhibit proliferation and activation of immune cells by the secretion of anti-inflammatory cytokines [4, 5].

The utilization of MSC immunomodulation properties in RA patients is supported by results of the anti-arthritic potentials of MSCs in an RA animal model [3, 6]. However, there are some gaps in the *in vivo* studies in terms of their limited therapeutic effect, worsening of symptoms, and highly variable efficacy after MSC administration [6—8]. In addition, whereas most of these studies were conducted with MSCs derived from mouse or non-patient specimens, investigations of the mechanisms of RA disease affected MSCs derived from disease regions or transplanted MSCs into disease regions, is a required for clinical evaluation of their therapeutic applications. Synovial fluid-derived MSCs (SF-MSCs) from RA patients are important for understanding pathogenesis, are easily obtained during the diagnosis or treatment of RA and have enhanced immunomodulation properties compared to bone marrow-derived MSCs (BM-MSCs) in collagen induced arthritis (CIA) mouse models [3, 9]. However, the distinctive characteristics of SF-MSCs in an arthritis milieu are not well understood and inflamed synovial fluid in a pathologic environment may result in alterations to the cells around inflammatory regions as the genotoxic stress, followed by a breakdown of the ability to recover injuries [3, 10, 11].

The comparative study of the immunomodulation properties of inflamed MSCs from RA patients is regarded as a prerequisite for understanding the RA disease-affected cellular mechanisms of MSCs and how they can be prepared for clinical applications in RA therapy. Given that SF-MSCs from RA patients (RA-SF-MSCs) have been exposed to the inflammation milieu, we hypothesized that the progression of cellular senescence and their potential of immunomodulation properties are affected by pathological events and cellular environmental factors of RA. Therefore, the present study aimed to uncover alterations in duration-dependent immunomodulation properties caused by inflammation-induced senescence in RA-SF-MSCs in an RA disease model.

Materials And Methods

Chemicals and Ethics used in experiments

All chemicals and media were purchased from Thermo (Waltham, MA, USA) or Sigma-Aldrich Chemical Company (St. Louis, MO, USA) unless otherwise specified. Collections of SF specimens and PBMCs were authorized by ‘GNUH 2012-05-009’ after obtaining informed consent from patients and volunteers. The protocol for animal experiments in CIA mice was approved by the Animal Center for Biomedical Experimentation at Gyeongsang National University (GNU-131209-M068).

Collection of SFs and establishment of SF-MSCs from RA patients

The control SFs were obtained from donors without evidence of inflammatory joint disease. The SFs for RA groups were obtained from the joints of RA patients who were divided into E-RA (disease duration < 2 years) or L-RA (disease duration > 10 years) groups, depending on how long they had been diagnosed with RA. Therefore, the SF-MSC were divided into three groups: CTL-SF-MSC (n = 10), E-SF-MSCs (n = 9) and L-SF-MSCs (n = 12). The clinical histories of RA patients are presented in Table 1. Cell isolation from the aspirated and cultured SFs were processed as previously described [3]. The SF specimens were filtered through a 40 μm nylon cell strainer (BD Falcon, NJ, USA) to remove debris and then cell pellets

were isolated by centrifugation at 400 × g for 10 min; the supernatants were stored at -80 °C until the inflammatory cytokine analysis. The resuspended cells were explanted onto 35 mm dishes (Nunc, Roskilde, Denmark) and allowed to adhere for 2 d in culture medium before non-adherent cells were discarded. The adherent cells were cultured with advanced Dulbecco's modified Eagle's medium (ADMEM) supplemented with 10% fetal bovine serum (FBS), 1% GlutaMax^{TM}, 10 ng/mL bFGF and 1% penicillin and streptomycin (10,000 IU and 10,000 μg/ml) at 36.5 °C in a humidified incubator with 5% CO_2. The expanded cells were taken through four passages before used for further analysis.

Characterization of SF-MSCs

Expression of MSC-specific cell surface molecules in SF-MSCs were validated with flow cytometry (BD FACS Calibur, NJ, USA) in triplicate. A total of 1 × 10^4 cells were harvested and were then fixed with 4% paraformaldehyde at 4 °C. All antibodies were diluted with 1% bovine serum albumin (1:200) (Table S1). The fluorescein isothiocyanate (FITC)-conjugated primary antibodies were incubated with the harvested cells for 1 h, with mouse IgG1-FITC used as an isotype control. Approximately ~80% of confluent SF-MSCs differentiated into adipocytes and osteoblasts after 3 w. Adipogenesis was induced with Dulbecco's modified Eagle's medium (DMEM) containing 10% FBS, 100 mM indomethacin, 10 mM insulin and 1 mM dexamethasone, and confirmed by intracellular lipid vacuoles staining with 0.5% Oil red O solution as well as gene expression (*FABP4* and *PPARγ*). Osteogenesis was induced with DMEM supplemented with 10% FBS, 200 mM ascorbic acid, 10 mM β-glycerophosphate, and 0.1 mM dexamethasone, and determined by the accumulation of calcium deposits visualized with 5% sliver nitrate solution (Von Kossa staining) and gene expression (*ON* and *OCN*). For chondrogenesis, 1 x 10^6 SF-MSCs were cultured for 3 w in 15 mL tubes containg STEMPRO Osteocyte/Chondrocyte basal medium supplemented with 10% chondrogenesis supplement. Cell pellets were then embedded in paraffin, cut into 5-mm sections and stained with 1% Alcian blue and 0.1% nuclear fast red solution counterstain to confirm synthesis of proteoglycans, as well as gene expression (*COL2* and *COL10A1*). The protocol for the gene expression analysis was described in a later section and primer information is displayed in Table S2.

Gene expression by quantitative PCR (q-PCR)

The q-PCR was used for gene expression studies to determine pluripotency (*Oct3/4*, *Sox2* and *Nanog*), apoptosis (*Bax, Bak, p53, Bcl2* and *Birc*), differentiation (*FABP4, PPARγ, ON, OCN, COL2* and *COL10A1*) and hypoxia-related genes (*GLUT1, LDHA, LOX* and *PGK1*). The q-PCR have three replicates of each sample and relevant primer information is displayed in Table S2. Total RNA was extracted using an RNeasy Minikit (Qiagen, CA, USA) and quantified using an OPTIZEN 3220 UV BIO spectrophotometer (Mecasys, Sungnam, Korea). Then, cDNA synthesis was performed from 1 mg total RNA using an Omniscript Reverse Transcription Kit (Qiagen) with an oligo dT primer at 60^{o}C for 1 h. The qRT-PCR was performed using a Rotor Gene Q qRT-PCR machine (Qiagen) with Rotor-Gene 2× SYBR Green mix (Qiagen) including 2 mL cDNA per reaction and 0.5 mM forward and reverse primers. The qPCR program settings included of pre-denaturation (95°C for 10 min), 45 PCR cycles (95°C for 10 s, 60°C for 6 s and 72°C for 4

s), melting curve analysis (60°C to 95°C by 1°C per 1 s) and cooling (40°C for 30 s). All transcriptional levels of target genes were normalized against *TBP* expression, which is known as a stable reference gene in human MSCs [12].

Proliferation and cell cycling in SF-MSCs

The Vybrant® MTT [3-(4,5-dimethylthiazol-2-yl)-2,5-diphenyltetrazolium bromide] Cell Proliferation Assay (Molecular Probes, Eugene, OR, USA) was used to evaluate the proliferation of SF-MSC cultures following the manufacture's protocol. Cell proliferation was quantified with an MTT colorimetric assay on a microplate reader (Molecular Devices) and absorbance of 540 nm. For the analysis of changes in the cell cycle, SF-MSCs were fixed with 70% ethanol, stained with 10 μg/ml propidium iodide (PI) solution and were analyzed using flow cytometry.

Senescence-associated β-galactosidase activity staining

Cellular senescence was evaluated using the Senescence *β*-Galactosidase Staining Kit (Cell Signaling Technology, Danvers, MA, USA). SF-MSCs were fixed for 15 min in fixation solution at room temperature and stained with β-Galactosidase staining solution, then incubated at 37°C overnight. For measurement of *β*-galactosidase activity, Mammalian β-Galactosidase Assay Kit (Thermo, Rockford, IL, USA) was used. SF-MSCs were harvested, added M-PER reagent for 10 min and centrifuged for 10 min at 27,000 x g. The supernatant was transferred into 96-well plate and treated the *β*-Galactosidase reagent for 30 minutes at 37°C. The optical density was determined at a wavelength of 405 nm using a microplate reader (Molecular Devices).

Evaluation of telomere length and telomerase activity

Telomere lengths of SF-MSCs were investigated using a nonradioactive chemiluminescent TeloTAGGG telomere restriction fragment (TRF) length assay kit (Roche, Indianapolis, IN, USA) following the manufacturer's instructions.

Suppression of PBMC proliferation by SF-MSCs

Human PBMCs were isolated from healthy donors (n = 6) with density gradient centrifugation using Ficoll-Paque™ PLUS (GE Healthcare, Uppsala, Sweden). PBMCs were then resuspended in RPMI 1640 complete medium supplemented with 10% FBS and 1% penicillin and streptomycin (10,000 IU and 10,000 μg/ml); cultures were stimulated with 1 μg/mL to activate T-cell proliferation. The PHAL-activated PBMCs (1×10^5 cells/well) were co-cultured for 5 d in a 96-well plate with three differentially conditioned pre-seeded SF-MSCs at PBMC:MSC ratios of 1:1, 1:2, and 1:4 before the addition of 5-bromo-2-deoxyuridine (BrdU). PBMC proliferation levels were performed using a Cell Proliferation ELISA, BrdU (colorimetric) Kit (Roche Diagnostics, Mannheim, Germany) according to the manufacturer's instructions.

Analysis of cytokine levels in SFs and SF-MSCs

The frozen SF supernatant samples were thawed and used to evaluate inflammatory cytokine levels. The levels of TNF-α and IL-1β in the SFs were determined with a Quantikine® ELISA kits (R&D Systems, Minneapolis, MN, USA) following the manufacturer's protocol. Briefly, standards and samples were incubated in wells pre-coated with the respective human primary antibody. The resulting antigen-antibody complex was detected using human TNF-α or IL-1β conjugated to horseradish peroxidase with preservatives, and the conjugate was quantified by a colorimetric reaction with a 3,3',5,5'-tetramethylbenzidine substrate. The resultant color intensity was read at 450 nm using a microplate reader (Molecular Devices). For SF-MSCs, 1×10^5 cells/well were cultured in 96 well plates in the serum-starvation medium (1% FBS ADMEM), followed by supplementation of human recombinant TNF-α (50 ng/mL; R&D Systems) for 2 d to activate inflammatory cytokine production. After collecting the supernatant, the levels of MMPs (MMP-1, MMP-3 and MMP-13) and other cytokines (IL-6 and IDO) were analyzed in the same manner as SFs. All samples were assayed in duplicate and the concentration of target proteins in each sample was determined by interpolation from the standard curve.

SF-MSCs administration to CIA mice

Injection of MSCs into collagen induced arthritis (CIA) mice was conducted following a previous publication [3]. Briefly, pathogen-free male DBA/1 mice (7-9-w-old; Orient Bio, Seoul, Korea) were immunized with 100 μl bovine type II collagen (Chondrex, Redmond, WA, USA) emulsified in complete Freund's adjuvant (CFA, Chondrex) by injection into the intradermal region of the tail on Day 0, and boosted by an equal volume of bovine type II collagen and incomplete Freund's adjuvant (IFA, Chondrex) on Day 21. The experiment included 4 groups (each n = 8), a PBS injection control and CTL-SF-MSCs, E-SF-MSCs, or L-SF-MSCs injected groups. SF-MSCs were intraperitoneally injected on Day 21 and repeated for five consecutive days with 200 mL PBS or the SF-MSC lines (5×10^6 cells per 200 μL PBS). The clinical arthritis scores (0-4 scale) were evaluated for each limb in accordance with a well-defined standard and had a total possible score of 16. To measure hind paw thickness, a caliper was placed across the ankle joint at the widest point to measure ankle thickness. On Day 48, CIA mice were humanely sacrificed by cervical dislocation. The hind paws were scanned by a SkyScan 1076 micro-CT apparatus (Bruker, Kontich, Belgium) and reconstructed into a three-dimensional structure with a voxel size of 18 μm using NRecon software and CT Analyzer (Bruker). Joint tissue specimens from CIA mice were fixed with 10% formalin, decalcified for 3-4 w in 10% EDTA, and embedded in a paraffin block. Joint sections (5 μm) were stained with hematoxylin and eosin (H&E), Safranin O or tartrate resistant acid phosphatase (TRAP) to evaluate articular inflammation, cartilage damage, and TRAP-positive multinucleated cells (osteoclast), respectively. The total number of TRAP-positive multinucleated cells containing three or more nuclei was counted in 10 areas of each CIA mouse ankle [3, 13].

Induction of the RA-like inflammation milieu

Because both low partial pressure of oxygen (hypoxia) and inflammation are relevant features in the synovial joints of RA patients [14], and *in vitro* RA-like inflammation milieu was induced in E-SF-MSCs to explore whether immunomodulation properties and senescence were altered in inflammation-exposed SF-

MSCs. The E-SF-MSCs were cultured in the normal culture condition for 3 d with an alteration in gas composition: 21% O_2, 5% CO_2 and 74% N_2 or 3% O_2, 5% CO_2 and 92% N_2 in a 95% humidified atmosphere, maintained in multi-gas incubators (ASTEC, Fukuoka, Japan) to the reflect normoxia or hypoxia, respectively. In addition, the media for hypoxic E-SF-MSCs were supplemented with 20 ng/mL TNF-α and 20 ng/mL IL-1β (R&D Systems) as the representative inflammatory cytokines. Both E-SF-MSCs and L-SF-MSCs under normoxic conditions were used as control counterparts.

Western blot analysis

The induction of hypoxia was validated by upregulation of HIF1α expression. The cell extracts of E-SF-MSCs with or without hypoxia were prepared with RIPA buffer supplemented with a Halt™ Protease Inhibitor Cocktail Kit (Pierce Biotechnology, Rockford, IL, USA). The concentration of total protein in the cell extracts was quantified using the Bicinchoninic Acid Protein Assay Reagent Kit (Pierce Biotechnology). A 25 μg aliquot from each sample was fractionated on a 10% SDS-PAGE by gel electrophoresis and was transferred onto a polyvinylidene difluoride membrane (Millipore, Darmstadt, Germany). The membranes were blocked with 0.1% bovine serum albumin (BSA), incubated with anti-HIF-1α or anti-GAPDH primary antibodies (1:100 dilution with BSA) at 4°C for overnight, incubated with horseradish peroxidase-conjugated secondary antibodies (1:3,000 dilution with BSA) at RT for 1 h, and detected using a chemiluminescence assay (Amersham Biosciences Corp, Piscataway, NJ, USA) with X-ray film for visualization.

Apoptosis assays

The proportion of apoptosis in E-SF-MSCs with or without induction of an RA-like inflammation milieu was determined using an Annexin V-FITC Apoptosis Detection Kit (Invitrogen, Eugene, OR, USA) following the manufacturer's instructions. From these cultures, 1×10^4 cells were harvested, washed twice in PBS, suspended with 200 μL binding buffer, treated with 10 μL Annexin V stock solution, incubated at 4°C for 30 min, counterstained with propidine iodide (PI), and analyzed using flow cytometry (BD FACS Calibur).

IDO activity measurements

The indoleamine 2,3-dioxygenase (IDO) activity was measured following a previous protocol [15]. Cultures were harvested and 2.5×10^4 E-SF-MSCs with or without induction of an RA-like inflammation milieu was cultured for 4 d and then supplemented with 100 μM L-Tryptophan (Sigma) for 4 h. The supernatant was then harvested from the cultures and 30% trichloroacetic acid (Sigma) was added before an additional incubation at 50°C for 30 min. This solution was diluted 1:1 in Ehrlich reagent (Sigma, USA) and the optical density was measured at 492 nm using a microplate reader (Molecular Devices). Serially diluted L-Kynurenine (Sigma) made with fresh culture medium was used as the standard.

Statistical analysis

The statistical significance was analyzed using paried T-test, one-way analysis of variance (ANOVA), and Tukey's multiple comparison test using SPSS 21.0 (IBM, Armonk, NY. USA) followed by Games-Howell post hoc analysis. All data were presented as mean ± Standard Deviation (SD). A value of $p < 0.05$ was considered as statistically significant difference.

Results

Normal Phenotype and Differentiation Property Exhibition of RA-SF-MSC Regardless of Disease Status

The RA patients were classified as early (E-RA) or long-standing (L-RA) RA in accordance with disease duration and degree of joint destruction, thus LRA patients had a longer disease duration and more severe joint destruction (modified sharp score) than E-RA (Table 1). Thus, three types of SF-MSCs were derived from healthy controls (CTL-SF-MSCs, n=10), ERA patients (E-SF-MSCs, n=9) and LRA patients (L-SF-MSCs, n=12) and established. All SF-MSCs presented normal MSC phenotypes such as plastic-adherent populations with fibroblastic morphology and positive MSCs-specific or -negative hematopoietic-specific cell surface molecule expressions (Figure 1A and 1B). Differentiation abilities of multi-mesenchymal lineages into adipocytes, osteoblasts and chondrocytes were also similar in all three types of SF-MSCs with an increase in lineage-specific gene expression (Figure 1C and 1D). Overall, we concluded that phenotype and differentiation ability of SF-MSCs were not reduced by the RA disease status.

Impaired Proliferation and Increased Senescence in L-SF-MSCs

The RA-SF-MSCs had lower proliferation ability with a slower cell cycle than CTL-SF-MSCs (Figure 2A and 2B). Telomere shortening, inactivation of telomerase and increased β-galactosidase activity (β-gal) were identified in L-SF-MSCs, indicating changed in cellular senescence patterns (Figure 2C and 2D). Moreover, inflammatory cytokine-treated L-SF-MSCs had a higher senescence-associated secretory phenotype (SASP) secretion than CTL-SF-MSCs and E-SF-MSCs (Figure 2E). In L-SF-MSCs, the expression of *Nanog*, a pluripotent factor in stem cells, and anti-apoptotic factors was lower and the expression of pro-apoptotic factors was higher than CTL-SF-MSCs (Figure 6). Collectively, these results suggest that L-SF-MSCs were more senescent than both CTL-SF-MSCs and E-SF-MSCs.

Reduced *in vitro* Immunomodulation Properties of L-SF-MSCs

Although all types of SF-MSCs were able to suppress peripheral blood mononuclear cell (PBMC) proliferation (Figure 3A), the intensity of this suppression varied depending on the groups (Figure 3B). Compared to the control group (PBMC + PHAL), the fold change of suppression of PBMC proliferation (PBMC:MSCs = 1:4) of CTL-SF-MSCs and L-SF-MSCs was significantly the most effective and the weakest, respectively. In addition, the secretion level of IDO in L-SF-MSCs post-treatment with TNF-α did not reach that of CTL-SF-MSCs (Figure 3C). Furthermore, IDO activity in L-SF-MSCs after IFN-γ treatment decreased more than that of CTL-SF-MSCs (Figure 3D). Overall, *in vitro* immunomodulation properties of L-SF-MSCs were attenuated more than in other SF-MSCs.

Attenuation of the Anti-Arthritic Properties of L-SF-MSCs in CIA Mice

The lower mean arthritis scores and ankle thickness of CIA mice injected with CTL- and E-SF-MSCs indicated the therapeutic effects of SF-MSCs; however, L-SF-MSC demonstrated no therapeutic potential and had worsening symptoms 44 d post-MSCs application (Figure 4A). The appearance of bone destructions did not progress in CTL- and E-SF-MSCs-injected CIA mice, but was detected in the joints of L-SF-MSCs-injected mice (Figure 4B). Whereas the joints of CIA mice post CTL- and E-SF-MSCs application histopathologically demonstrated prevention of arthritis, those injected with L-SF-MSCs presented arthritis-related changes such as synovial inflammation, cartilage damage, and osteoclast cell activity (Figure 4C). Based to these *in vitro* and *in vivo* results, we conclude that the preventative effects of SF-MSCs are varied and depend on disease duration. Furthermore, L-SF-MSCs almost lost their immunomodulation properties, possibly due to prolonged exposure to the RA inflammation milieu.

Cellular Alteration of E-SF-MSCs into L-SF-MSCs in the RA-mimic Milieu

The synovial tissues of RA patients are exposed to the inflammation milieu, including both inflammatory cytokines and hypoxia [14]. In particular, L-SF-MSCs derived from the SF of LRA patients have been exposed to prominent pro-inflammatory cytokines for a longer time than E-SF-MSCs (Figure S1). Therefore, we asked whether an RA joint-mimicking milieu with the treatment of inflammatory cytokines and hypoxia (h+/i+) could provoke cellular and immunomodulatory alterations in E-SF-MSCs when compared with non-treated L-SF-MSCs (h-/i- L-SF-MSCs). This experiment will clarify the effect of the chronic inflammation milieu on RA-SF-MSCs. The exposure of E-SF-MSCs to hypoxia was validated by the increase of hypoxia-inducible factor (HIF)-1α and downstream signaling cascades (Figure 5A), whereas the induction of apoptosis and cellular senescence was demonstrated in h+/i+ E-SF-MSCs in the RA joint-mimicking milieu, but not non-treated E- and hypoxic E-SF-MSCs (h-/i- and h+/i- E-SF-MSCs) (Figure 5B and C). Although h+/i+ E-SF-MSCs maintained IDO activity and the ability to suppress PBMC proliferation as immunomodulation properties, the intensities of these activities were weaker than in h+/i- E-SF-MSCs (Figure 5D). Interestingly, the levels of these changes in h+/i+ E-SF-MSCs were similar to those measured in h-/i- L-SF-MSCs, suggesting that the chronic inflammation milieu of the joints of LRA patients influenced the status of MSC cellular senescence and immunomodulation properties.

Discussion

MSCs display a remarkable potential for immunomodulation properties as a cell-based regimen for inflammatory disease; however, accurate understanding for the therapeutic mechanism of MSCs and their different characteristics during disease are particularly important to the development of safe and effective therapeutic strategies. The present study demonstrates the presence of SF-MSC populations in RA patients regardless of disease duration and uncovers that immunomodulation properties of RA-SF-MSCs are attenuated due to inflammation-induced senescence in the inflammatory milieu of RA joints. The immunomodulation properties of RA-SF-MSCs is especially altered in an RA disease duration-dependent manner. Therefore, the present findings suggest that the therapeutic effects of disease-

affected MSCs on autoimmune disease are highly associated with pathology and cellular environmental factors.

The significant populations of MSCs collected from SFs of arthritic patients have been clearly addressed in the previous research. In the study of mesenchymal progenitor cells (MPCs) obtained from RA patients, there were no significant differences between the number of MPCs in the SFs from ERA and LRA patients or in characteristics such as differentiation ability and phenotypes [16]. Consistent with this result, the presence of MSCs in SFs from RA patients were identified through characterization of the minimal criteria for MSCs defined by the International Society of Cellular Therapy (Figure 1) [17]. However, our results provide clear evidence for progression of cellular senescence in RA-SF-MSCs in an RA disease duration-dependent manner; as shown by elevated β-galactosidase positive cell populations, shortened telomere length, attenuated telomerase activity, apoptosis-related gene expression, and drastic enhancement of SASPs secretions in L-SF-MSCs exposed to inflammatory cytokines for a longer time compared to CTL- and E-SF-MSCs (Figures 2, 6 and S1). Cellular senescence is activated during intrinsic stress such as extensive cell replication and/or extrinsic stress like ultraviolet radiation, oxidative damage, activated oncogenes, and chronic inflammation. In particular, during chronic inflammation that occurs with liver cirrhosis, hematopoietic stem cell-associated disorders, chronic human immunodeficiency virus (HIV) infection, myelodysplastic syndromes, ulcerative colitis and LRA, immune cells produce strong oxidizing genotoxic substances that are able to induce the cellular senescence [18-21]. In the inflammation milieu, pro-inflammatory cytokines are produced from stimulated lymphocytes by antigens or pathogens and activate immune cells, inhibit proliferation of transformed cells and intensify anti-viral/-tumor effects on cells; moreover, they also induce cellular senescence in diverse kinds of cells including melanocytes, endothelial cells and MSCs [10, 21-25]. Because cellular senescence is defined as the irreversible changes that inhibit cellular division, growth, and function, senescent MSCs from an experimentally-induced model as well as RA and systemic lupus erythematosus (SLE) patients exhibit degradation of distinct cellular features, including differentiation potential, immunomodulation properties, misregulation of pro-inflammatory cytokine production and reduction in migratory ability [2, 5, 10, 11, 19, 21, 23-28]. Therefore, these studies cumulatively show that the chronic inflammation milieu of LRA is closely associated with inducing the cellular senescence in L-SF-MSCs.

Because MSCs modulate the immune response of both the adaptive and innate immune systems, there is an interest in using them to develop new cell-based therapeutic approaches for the treatment of various inflammatory diseases [5, 29]. The immunomodulation properties of MSCs are not spontaneously acquired but are initiated when they are primed through exposure to pro-inflammatory cytokines and secretion of anti-inflammatory factors that have inhibitory effects on immune cells [26, 30, 31]. Therefore, administration of MSCs has demonstrated improvements on the clinical signs associated with autoimmune encephalomyelitis, autoimmune diabetes, multiple sclerosis, polymyositis, atopic dermatitis and RA [32-34]. Indeed, pre-clinical research of MSCs applications for RA treatment have been actively conducted to clarify the pathogenesis of arthritis and the therapeutic mechanisms of MSCs using CIA and antigen-induced arthritis (AIA) mice strains. MSC-injected CIA or AIA mice display a reduction in inflammation, prevention of cartilage destruction, integration of injected MSCs into the synovium,

amelioration of inflammation-induced systemic bone erosion, reduction of osteoclast precursors, inhibition of receptor activator of NF-κB ligand (RANKL)-induced osteoclastogenesis, elevation of anti-inflammatory cytokines, and suppression of pro-inflammatory cytokines [3, 35, 36]. However, in the present study, we verified that SF-MSCs did not have the same immunomodulation properties (Figures 3 and 4). While CTL-SF-MSCs demonstrated intensive suppression of PBMC proliferation and significant anti-arthritic effects in mice, the immunomodulation properties of RA-SF-MSCs were attenuated depending on RA disease status. Moreover, several articles have suggested that MSCs were incapable of therapeutically modulating arthritis in CIA mice [6-8]. When considering these and our current results, environmental parameters such as the MSC administration route, the degree of the inflammation milieu and/or the condition of the MSCs could influence their immunomodulation properties. Because L-SF-MSCs used in the present study were directly exposed in the inflammation milieu for 13.8 years (Figure S1), we further investigated whether the genotoxic stress caused by chronic inflammation in LRA patients could alter the characteristics and senescence status of RA-SF-MSCs.

The synovial tissues, including SFs, of RA patients are characterized by both chronic inflammation and hypoxic regions compared to those of osteoarthritis and healthy patients. These symptoms are due to an increase in oxygen consumption by metabolically active tissue because of formation of the pannus mass and recruitment of inflammatory cells, as well as newly formed and immature vessels (angiogenesis) that cannot supply enough oxygen to the tissue [14, 37-40]. In addition, hypoxia can especially alter mitochondrial activity and increase ROS production and oxidative damage to the inflamed tissues in RA, potentially inducing senescence of cells in response to the genotoxic substances [38]. Likewise, both hypoxia-conditioned E-SF-MSCs (h+/i- E-SF-MSCs) and non-treated E-SF-MSCs (h-/i- E-SF-MSCs) demonstrated maintenance of immunomodulation properties and non-senescent status; while E-SF-MSCs in an RA joint-mimicking milieu with hypoxia and pro-inflammatory cytokines (h+/i+ E-SF-MSCs) exhibited senescence-related cellular effects, including increased apoptosis, telomere shortening, elevated *β*-galactosidase activity, and attenuation of the immunomodulation properties IDO activity and inhibition of PBMC proliferation), which were similar to observations made in non-treated L-SF-MSCs (h-/i- L-SF-MSCs) (Figure 5). Therefore, it is likely that the chronic inflammation milieu with hypoxia and pro-inflammatory cytokines in inflamed RA joints causes genotoxic stress in RA that increases over time, indicating that RA-SF-MSCs have limited immunomodulation properties at the inflamed site due to inflammation-induced senescence.

Conclusion

In conclusion, we characterized and investigated the how the immunomodulation properties of RA-SF-MSCs change in response to disease duration. To our knowledge, the present study is the first effort to comparatively evaluate the cellular senescence and immunomodulation characteristics of SF-MSCs under different inflammation milieus. The three types of SF-MSCs derived from RA patients with different disease prognoses were well verified by the differentiation ability and expression of MSC-specific cell surface molecules. Although both E- and L-SF-MSCs were exposed to the inflammation milieu of RA, the immunomodulation properties in CIA mice was attenuated depending on disease progression. Cellular

senescence was induced by long term exposure to chronic inflammation and was considered to be one reason that L-SF-MSCs had decreased immunomodulation properties. Therefore, since the fate and potential of MSCs depends on their exposure to the inflammatory environment, consideration of inflammation duration is required prior to the initiation of autologous stem cell application for inflammatory disease treatment or for the clinical application of inflammatory stem cells.

Abbreviations

MSCs: Mesenchymal stem cells; RA: Rheumatoid arthritis; SF: synovial fluid; SF-MSCs: Synovial fluid-derived MSCs; RA-SF-MSCs: SF-MSCs from RA patients; E-SF-MSCs: MSCs derived from synovial fluid of early RA patients; L-SF-MSCs: MSCs derived from synovial fluid of long-standing RA patients; CTL-SF-MSCs: MSCs derived from synovial fluid of healthy controls; CIA: Collagen induced arthritis; BM-MSCs: Bone marrow-derived MSCs; ADMEM: Advanced Dulbecco's modified Eagle's medium; FBS: fetal bovine serum; FITC: fluorescein isothiocyanate; DMEM: Dulbecco's modified Eagle's medium; PI: Propidium iodide; TRF: Telomere restriction fragment; PHAL: Phytohemagglutinin-L; BrdU: 5-bromo-2-deoxyuridine; H&E: Hematoxylin and eosin; TRAP: Tartrate resistant acid phosphatase; β-gal: β-galactosidase activity; SASP: Senescence-associated secretory phenotype; PBMC: Peripheral blood mononuclear cell; IDO: Indoleamine 2,3-dioxygenase; MPCs: Mesenchymal progenitor cells; HIV: Human immunodeficiency virus; SLE: systemic lupus erythematosus; AIA: Antigen-induced arthritis; RANKL: Receptor activator of NF-κB ligand; TRF: Telomere restriction fragment; RTA: Relative telomerase activity; MMPs: Matrix metalloproteinases family; BS/BV: Bone surface/bone volume

Declarations

Acknowledgments

Not applicable

Author contributions

H.-J.L.: conception and design, collection and assembly of data, data analysis and interpretation, manuscript writing; W.-J.L: conception and design, collection and assembly of data, data analysis and interpretation, manuscript writing; S.-C.H.: administrative support, provision of study material or patients; Y.-H.C., S.K., E.B. and S.L.: collection and assembly of data, data analysis and interpretation; S.-J.K.: administrative support; H.-O.K.: administrative support, provision of study material or patients; S.-A.O.: administrative support; H.-S.N.: collection and assembly of data, data analysis and interpretation; G.-J.R.: financial support, conception and design; S.-I.L.: financial support, conception and design, provision of study material or patients, manuscript writing; S-L.L.: financial support, conception and design, final approval of manuscript

Funding

This study was supported by a grant from the Korea Health Technology R&D project through the Korea Health Industry Development Institute (KHIDI) funded by the Korean Ministry of Health and Welfare (grant number: HI14C1277) and the National Research Foundation (NRF) of Korea, funded by the government of the Republic of Korea (grant no. NRF- 2018R1D1A3B07048602).

Availability of data and materials

Main data have been listed in the primary figures and supplemental data. All the original data are available from the corresponding author on reasonable request.

Ethics approval and consent to participate

All work was performed within the guidelines of the Gyeongsang National University School of Medicine and Hospital, and collections of SF specimens and PBMCs were authorized by 'GNUH 2012-05-009' after obtaining informed consent from patients and volunteers. The protocol for animal experiments in CIA mice was approved by the Animal Center for Biomedical Experimentation at Gyeongsang National University (GNU-131209-M068).

Consent for publication

Not applicable.

Competing interests

The authors declare that they have no competing interests.

Author details

[1]College of Veterinary Medicine, Gyeongsang National University, Jinju, 52828 Republic of Korea. [2]College of Veterinary Medicine, Kyungpook National University, Daegu, 41566 Republic of Korea. [3]Department of Orthopaedic Surgery, Gyeongsang National University School of Medicine and Hospital, Jinju, 52727 Republic of Korea. [4]Department of Internal Medicine and Institute of Health Sciences, Gyeongsang National University School of Medicine and Hospital, Jinju, 52727 Republic of Korea. [5]Animal Biotechnology Division, National Institute of Animal Science, Rural Development Administration, 1500 Kongjwipatjwi-ro, Isero-myeon, Wanju-gun, Jeollabuk-do 565-851, Republic of Korea. [6]Research Institute of Life Sciences, Gyeongsang National University, Jinju, 52828 Republic of Korea

References

1. Gonzalez-Rey E, Gonzalez MA, Varela N, O'Valle F, Hernandez-Cortes P, Rico L, et al. Human adipose-derived mesenchymal stem cells reduce inflammatory and T cell responses and induce regulatory T cells in vitro in rheumatoid arthritis. Ann Rheum Dis. 2010;69(1):241-8.

2. Papadaki HA, Kritikos HD, Gemetzi C, Koutala H, Marsh JC, Boumpas DT, et al. Bone marrow progenitor cell reserve and function and stromal cell function are defective in rheumatoid arthritis: evidence for a tumor necrosis factor alpha-mediated effect. Blood. 2002;99(5):1610-9.
3. Lee WJ, Hah YS, Ock SA, Lee JH, Jeon RH, Park JS, et al. Cell source-dependent in vivo immunosuppressive properties of mesenchymal stem cells derived from the bone marrow and synovial fluid of minipigs. Exp Cell Res. 2015;333(2):273-88.
4. Krampera M, Cosmi L, Angeli R, Pasini A, Liotta F, Andreini A, et al. Role for interferon-gamma in the immunomodulatory activity of human bone marrow mesenchymal stem cells. Stem Cells. 2006;24(2):386–98.
5. Turinetto V, Vitale E, Giachino C. Senescence in Human Mesenchymal Stem Cells: Functional Changes and Implications in Stem Cell-Based Therapy. Int J Mol Sci. 2016;17(7):1164.
6. Djouad F, Fritz V, Apparailly F, Louis-Plence P, Bony C, Sany J, et al. Reversal of the immunosuppressive properties of mesenchymal stem cells by tumor necrosis factor alpha in collagen-induced arthritis. Arthritis Rheum. 2005;52(5):1595-603.
7. Chen B, Hu J, Liao L, Sun Z, Han Q, Song Z, et al. Flk-1+ mesenchymal stem cells aggravate collagen-induced arthritis by up-regulating interleukin-6. Clin Exp Immunol. 2010;159(3):292-302.
8. Schurgers E, Kelchtermans H, Mitera T, Geboes L, Matthys P, et al. Discrepancy between the in vitro and in vivo effects of murine mesenchymal stem cells on T-cell proliferation and collagen-induced arthritis. Arthritis Res Ther. 2010;12(1):R31.
9. Sekiya I, Ojima M, Suzuki S, Yamaga M, Horie M, Koga H, et al. Human mesenchymal stem cells in synovial fluid increase in the knee with degenerated cartilage and osteoarthritis. J Orthop Res. 2012;30(6):943-9.
10. Kim KS, Kang KW, Seu YB, Baek SH, Kim JR. Interferon-gamma induces cellular senescence through p53-dependent DNA damage signaling in human endothelial cells. Mech Ageing Dev. 2009;130(3):179-88.
11. Davalos AR, Coppe JP, Campisi J, Desprez PY. Senescent cells as a source of inflammatory factors for tumor progression. Cancer Metastasis Rev. 2010;29(2):273-283.
12. Ragni E, Viganò M, Rebulla P, Giordano R, Lazzari L. What is beyond a qRT-PCR study on mesenchymal stem cell differentiation properties: how to choose the most reliable housekeeping genes. J Cell Mol Med. 2013;17(1):168-80.
13. Lee HS, Woo SJ, Koh HW, Ka SO, Zhou L, Jang KY, et al. Regulation of apoptosis and inflammatory responses by insulin-like growth factor binding protein 3 in fibroblast-like synoviocytes and experimental animal models of rheumatoid arthritis. Arthritis Rheumatol. 2014;66(4):863-73.
14. Quiñonez-Flores CM, González-Chávez SA, Pacheco-Tena C. Hypoxia and its implications in rheumatoid arthritis. J Biomed Sci. 2016;23(1):62.
15. Roemeling-van Rhijn M, Mensah FK, Korevaar SS, Leijs MJ, van Osch GJ, Ijzermans JN, et al. Effects of Hypoxia on the Immunomodulatory Properties of Adipose Tissue-Derived Mesenchymal Stem cells. Front Immunol. 2013;18(4):203.

16. Jones EA, English A, Henshaw K, Kinsey SE, Markham AF, Emery, P, et al. Enumeration and phenotypic characterization of synovial fluid multipotential mesenchymal progenitor cells in inflammatory and degenerative arthritis. Arthritis Rheum. 2004;50(3):817-27.
17. Dominici M, Le Blanc K, Mueller I, Slaper-Cortenbach I, Marini F, Krause D, et al. Minimal criteria for defining multipotent mesenchymal stromal cells. The International Society for Cellular Therapy position statement. Cytotherapy. 2006;8(4):315-7.
18. Tümpel S, Rudolph KL. The role of telomere shortening in somatic stem cells and tissue aging: lessons from telomerase model systems. Ann N Y Acad Sci. 2012;1266:28-39.
19. Kastrinaki MC, Sidiropoulos P, Roche S, Ringe J, Lehmann S, Kritikos H, et al. Functional, molecular and proteomic characterisation of bone marrow mesenchymal stem cells in rheumatoid arthritis. Ann Rheum Dis. 2008;67(6):741-9.
20. Loeser RF. Aging and osteoarthritis: the role of chondrocyte senescence and aging changes in the cartilage matrix. Osteoarthritis Cartilage. 2009;17(8):971-9.
21. Yang ZX, Mao GX, Zhang J, Wen XL, Jia BB, Bao YZ, et al. IFN-γ induces senescence-like characteristics in mouse bone marrow mesenchymal stem cells. Adv Clin Exp Med. 2017;26(2):201-6.
22. Wang S, Zhou M, Lin F, Liu D, Hong W, Lu L, et al. Interferon-γ induces senescence in normal human melanocytes. PLoS One. 2014;9(3):e93232.
23. Krüger JP, Endres M, Neumann K, Stuhlmüller B, Morawietz L, Häupl T, et al. Chondrogenic differentiation of human subchondral progenitor cells is affected by synovial fluid from donors with osteoarthritis or rheumatoid arthritis. J Orthop Surg Res. 2012;13(7):10.
24. Zhang J, Li ZG, Si YM, Chen B, Meng J, et al. The difference on the osteogenic differentiation between periodontal ligament stem cells and bone marrow mesenchymal stem cells under inflammatory microenviroments. Differentiation. 2014;88(4-5):97-105.
25. Valencic E, Loganes C, Cesana S, Piscianz E, Gaipa G, Biagi E, et al. Inhibition of mesenchymal stromal cells by pre-activated lymphocytes and their culture media. Stem Cell Res Ther. 2014;5(1):3.
26. Sepúlveda JC, Tomé M, Fernández ME, et al. Cell senescence abrogates the therapeutic potential of human mesenchymal stem cells in the lethal endotoxemia model. Stem Cells. 2014;32(7):1865-1877.
27. Jones E, Churchman SM, English A, Delgado M, Campisi J, Bernad A, et al., Mesenchymal stem cells in rheumatoid synovium: enumeration and functional assessment in relation to synovial inflammation level. Ann Rheum Dis. 2010;69(2):450-7.
28. Li X, Liu L, Meng D, Wang D, Zhang J, Shi D, et al. Enhanced apoptosis and senescence of bone-marrow-derived mesenchymal stem cells in patients with systemic lupus erythematosus. Stem Cells Dev. 2012;21(13):2387-94.
29. Keating A. Mesenchymal stromal cells: new directions. Cell Stem Cell. 2012;10(6):709-16.
30. Mazzanti B, Aldinucci A, Biagioli T, Barilaro A, Urbani S, Dal Pozzo S, et al. Differences in mesenchymal stem cell cytokine profiles between MS patients and healthy donors: implication for assessment of disease activity and treatment. J Neuroimmunol. 2008;199(1-2):142-50.

31. Glennie S, Soeiro I, Dyson PJ, Lam EW, Dazzi F, Bone marrow mesenchymal stem cells induce division arrest anergy of activated T cells. Blood. 2005;105(7):2821–7.
32. Lee RH, Seo MJ, Reger RL, Spees JL, Pulin AA, Olson SD, et al. Multipotent stromal cells from human marrow home to and promote repair of pancreatic islets and renal glomeruli in diabetic NOD/scid mice. Proc Natl Acad Sci USA. 2006;103(46):17438-43.
33. Zappia E, Casazza S, Pedemonte E, Benvenuto F, Bonanni I, Gerdoni E, et al. Mesenchymal stem cells ameliorate experimental autoimmune encephalomyelitis inducing T-cell anergy. Blood. 2005;106(5):1755-61.
34. Ra JC, Kang SK, Shin IS, Park HG, Joo SA, Kim JG, et al. Stem cell treatment for patients with autoimmune disease by systemic infusion of culture-expanded autologous adipose tissue derived mesenchymal stem cells. J Transl Med. 2011;21(9):181.
35. Kehoe O, Cartwright A, Askari A, El Haj AJ, Middleton J. Intra-articular injection of mesenchymal stem cells leads to reduced inflammation and cartilage damage in murine antigen-induced arthritis. J Transl Med. 2014;3(12):157.
36. Garimella MG, Kour S, Piprode V, Mittal M, Kumar A, Rani L, et al. Adipose-Derived Mesenchymal Stem Cells Prevent Systemic Bone Loss in Collagen-Induced Arthritis. J Immunol. 2015;195(11):5136-48.
37. Lee YA, Kim JY, Hong SJ, Lee SH, Yoo MC, Kim KS, et al. Synovial proliferation differentially affects hypoxia in the joint cavities of rheumatoid arthritis and osteoarthritis patients. Clin Rheumatol. 2007;26(12): 2023-9.
38. Fearon U, Canavan M, Biniecka M, Veale DJ. Hypoxia, mitochondrial dysfunction and synovial invasiveness in rheumatoid arthritis. Nat Rev Rheumatol. 2016;12(7):385-97.
39. Stevens CR, Blake DR, Merry P, Revell PA, Levick JR. A comparative study by morphometry of the microvasculature in normal and rheumatoid synovium. Arthritis Rheum. 1991;34(12):1508-13.
40. Taylor PC, Sivakumar B. Hypoxia and angiogenesis in rheumatoid arthritis. Curr Opin Rheumatol. 2005;17(3):293-8.

Tables

Table 1: Demographic and disease characteristics of donors

Characteristics	C-SF-MSCs (n=10)	E-RA-SF-MSCs (n=9)	L-RA-SF-MSCs (n=12)	*P* value*
Age (years)	23.0 (1.22)	55.4 (14.1)	58.5 (8.6)	-
Women	3 (30%)	8 (88.8%)	12 (100%)	-
Positive for rheumatoid factor	-	8 (88.8%)	12 (100%)	-
Positive for anti-CCP antibody	-	8 (88.8%)	12 (100%)	-
DAS28-ESR	-	5.1 (1.4)	4.6 (1.1)	-
Disease duration (years)	-	1.7 (1.1)	13.8 (5.1)	0.011
Modified Sharp score	-	7.9 (8.8)	49.7 (26.4)	0.015

Data are means (SE) or n (%), *P value indicates E-SF-MSC vs. L-SF-MSC. C-SF, control synovial fluid; ERA or LRA, early or long-standing rheumatoid arthritis; MSC, mesenchymal stem cell; CCP, cyclic citrullinated peptide; DAS28-ESR, disease activity score 28-erythrocyte sediment rate

Figures

Figure 1.

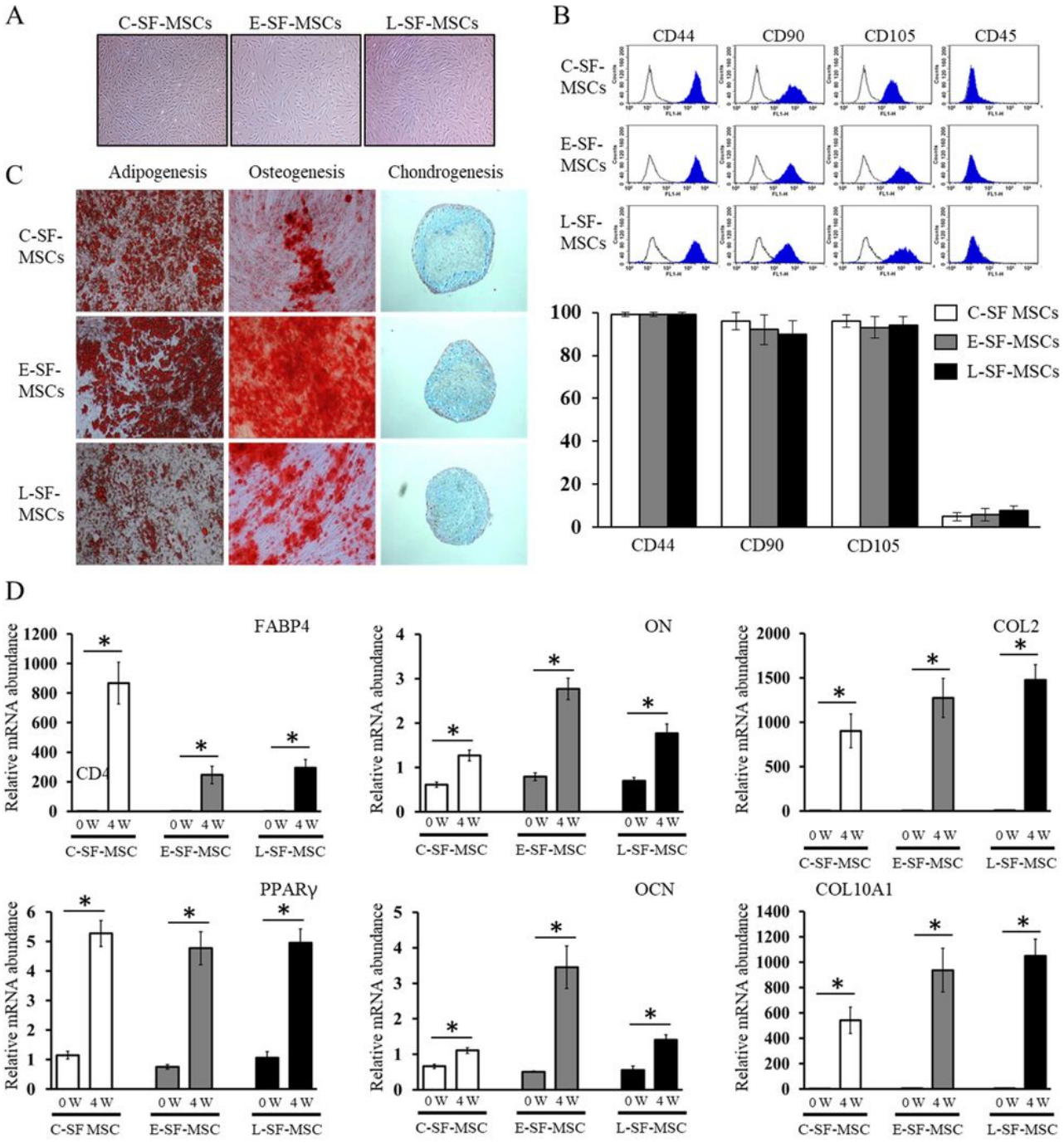

Figure 1

Characteristics and differentiation abilities of RA patient-derived SF-MSCs depends on disease duration. (A) The plastic-adherent population with fibroblastic morphology; (B) flow cytometry indicates the positive expression of MSC-specific molecules (CD44, CD90 and CD105) and negative expression of hematopoietic cell surface molecule (CD45) within this SF-MSC population. (C) Cytochemical staining of differentiated SF-MSCs toward adipocytes (lipid droplets), osteoblasts (calcium deposit) and

chondrocytes (proteoglycan synthesis) when grown in vitro; and (D) changes in lineage-specific gene expression. The asterisks indicate significant differences. The graphs present as percentage mean values ± SD. Magnification × 40. 0W, undifferentiated SF-MSCs at the start of the culture; 4W, differentiated SF-MSCs for 4 W.

Figure 2.

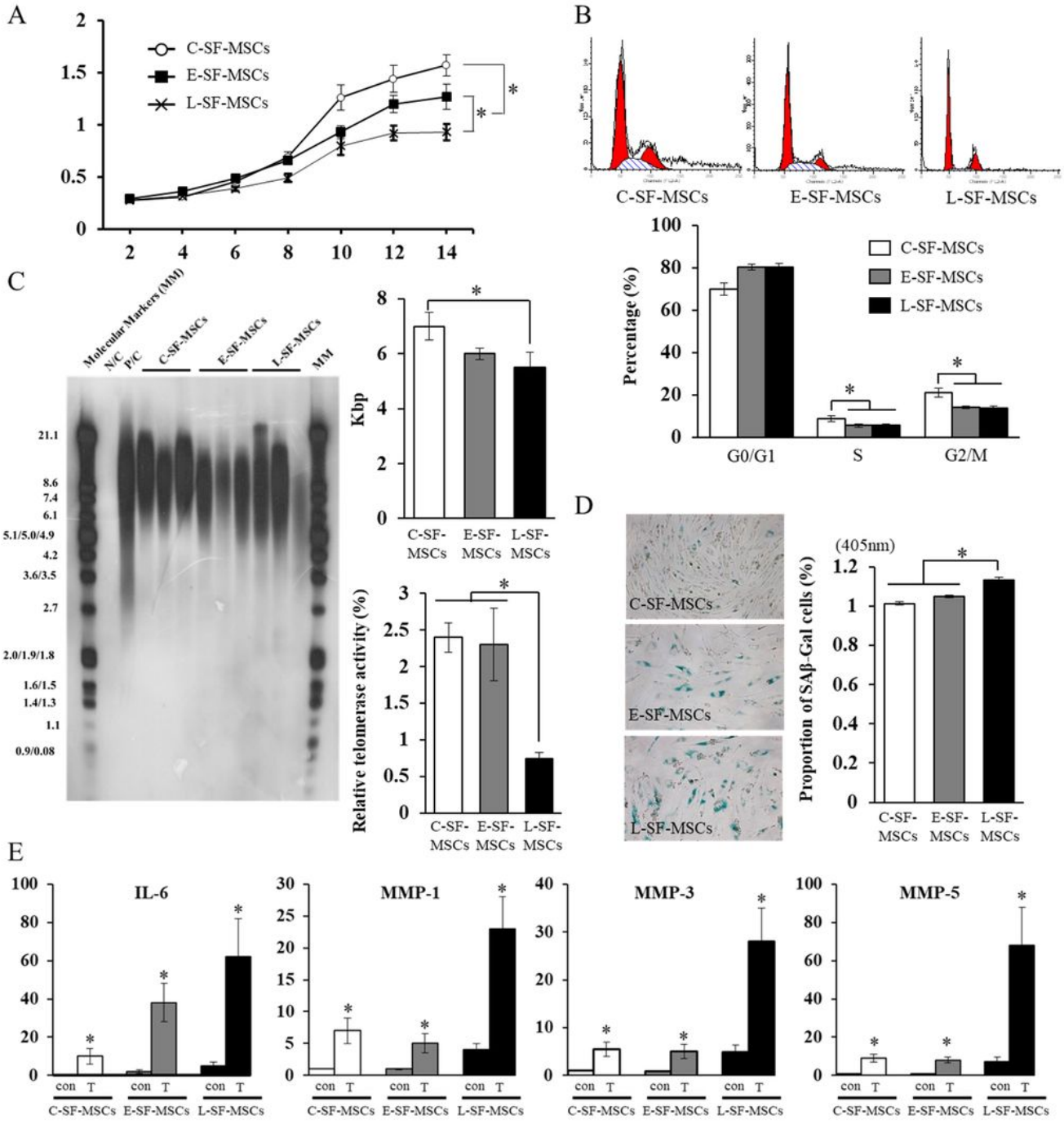

Figure 2

Proliferative ability and cellular senescence of RA patient-derived SF-MSCs. (A) Comparison of proliferation SF-MSCs by MTT assay. (B) Cell cycle status of SF-MSCs by flow cytometry. (C)The range of telomere restriction fragment (TRF) lengths (Kbp) in SF-MSCs by non-radioactive chemiluminescent. (D) Evaluation of the relative telomerase activity (RTA) in SF-MSCs by qRT-PCR. (E) Comparison of β-galactosidase positive cell populations in SF-MSCs. Magnification × 100. (F) ELISA quantification of SASP secretion level after treatment with inflammatory cytokines. T or Con indicates the groups that did or did not receive inflammatory cytokine treatment, respectively. The asterisks indicate significant differences. The graphs are presented as mean values ± SD. N/C, negative control; P/C, positive control; SA β-gal, senescence-associated β-galactosidase; SASP, senescence associated secretory phenotype; MMPs, matrix metalloproteinases family.

Figure 3.

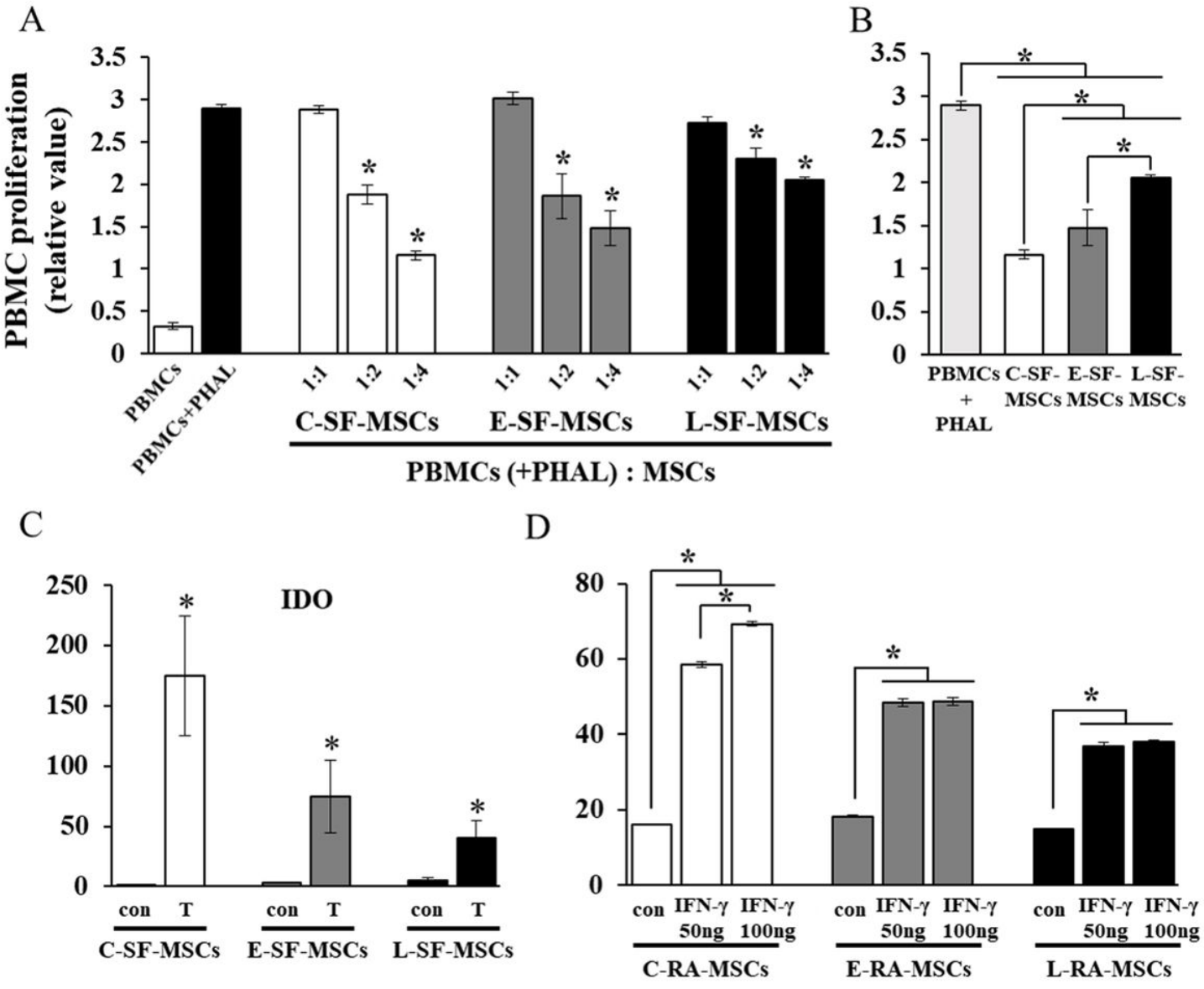

Figure 3

In vitro immunomodulation properties of RA patient-derived SF-MSCs. (A) Evaluation of PBMC proliferation inhibition. The ratios 1:1, 1:2 and 1:4 indicate the cell population of pre-seeded SF-MSCs against PBMC. PBMC or PBMC+PHAL indicate the PBMC cultures without or with PHAL, respectively. (B) Comparison of PBMC proliferation inhibition intensity in the highest PBMC:MSCs ratio (1:4). (C) Quantification of IDO secretion levels after treatment with inflammatory cytokines by ELISA. Con or T indicate cells that were untreated or treated with inflammatory cytokine, respectively. (D) Evaluation of IDO activity after treatment with IFN-γ by measurement of L-Kynurenine. The asterisks indicate significant differences. The graphs are presented as mean value ± SD. PBMC, peripheral blood mononuclear cells; PHAL, phytohemagglutinin-L; IDO, indoleamine 2,3-dioxygenase; IFN-γ, interferon-γ.

Figure 4.

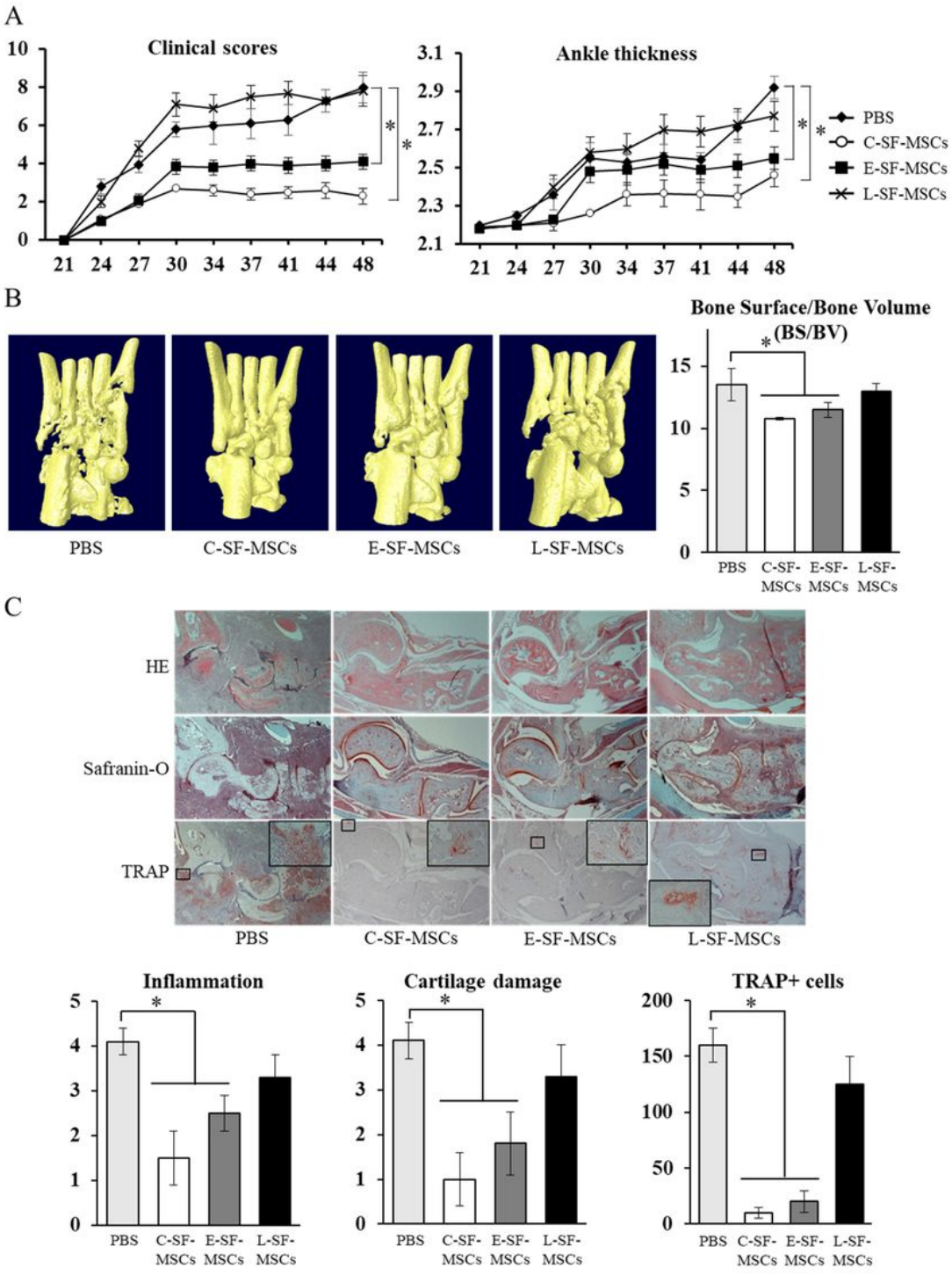

Figure 4

In vivo anti-arthritic potential of RA patient-derived SF-MSCs. (A) Evaluation of the clinical scores and measurements of hind paw thickness in CIA mice after the intraperitoneal administration of SF-MSCs or PBS. (B) Images of micro CT scanning and analysis of bone surface/bone volume (BS/BV) analysis. (C) Histological examination of therapeutic effects of SF-MSCs. Magnification × 40 or × 200. Graphs summarize the scoring of the pathological manifestations in terms of inflammation, cartilage damage

and TRAP + cell (osteoclast) population of the joint from CIA mouse. The asterisks indicate significant differences. The graphs present as the mean values ± SD. PBS, phosphate-buffered saline; H&E, hematoxylin and eosin; TRAP, tartrate resistant acid phosphatase.

Figure 5.

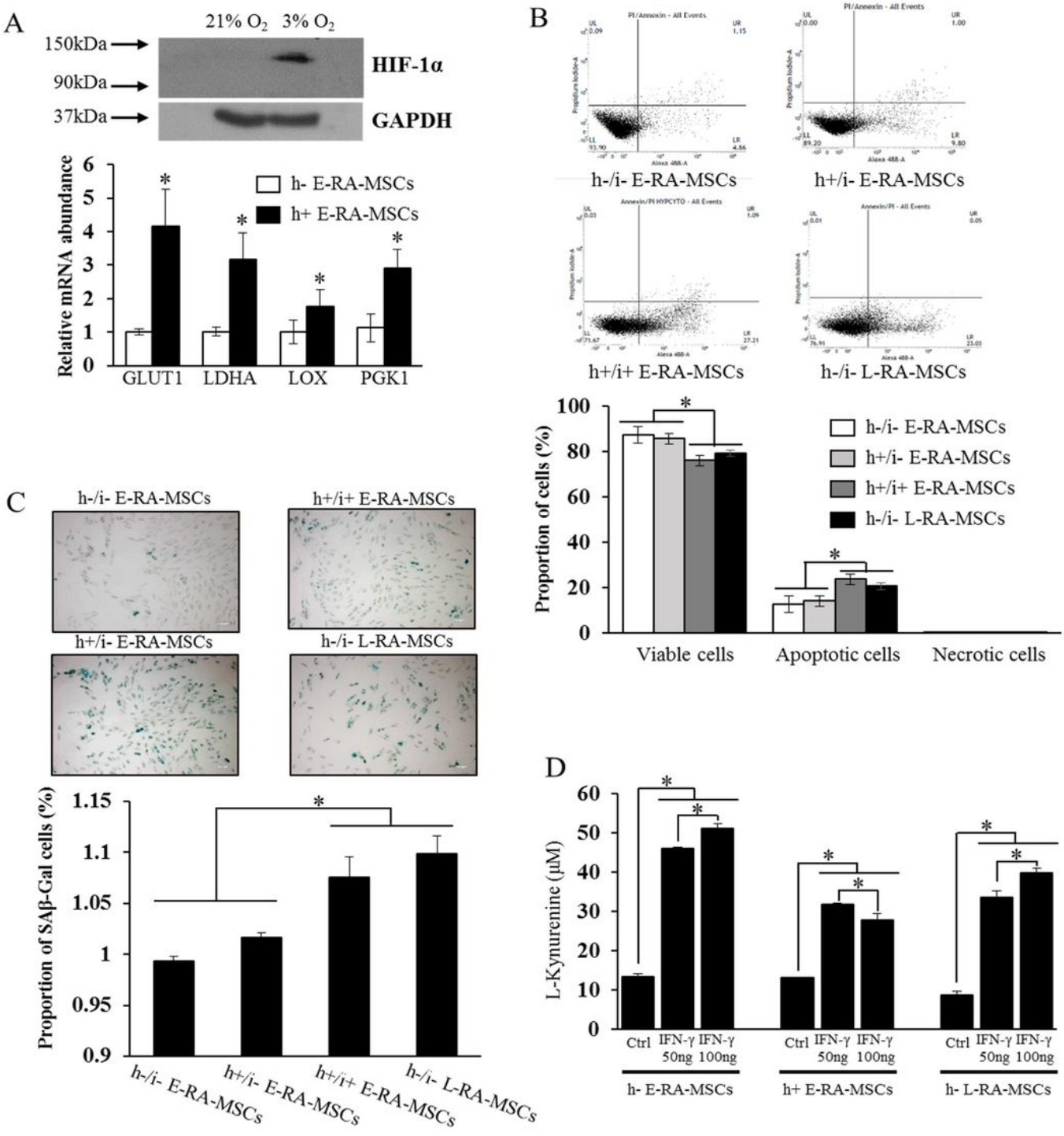

Figure 5

Alteration of cellular senescence of SF-MSC by the long-standing RA-mimic milieu. (A) Confirmation of hypoxic culture conditions in E-SF-MSCs by western blotting and qRT-PCR. 21% O2 or 3% O2 indicate

normoxic or hypoxic culture conditions in SF-MSCs, respectively. (B) Measurement of the apoptosis in SF-MSCs with or without induction of the RA joint-mimicking milieu using flow cytometry with Annexin V/PI staining. Cells with Annexin V-/PI- or Annexin V-/PI+ or Annexin V+/PI- with V+/PI+ staining were alive, necrotic or apoptotic, respectively. (C) The range of TRF lengths (Kbp) in SF-MSCs with or without induction of the RA joint-mimicking milieu by Southern blotting. (D) Comparison of positive β-gal cell populations in SF-MSCs with or without induction of the RA joint-mimicking milieu. (E) Evaluation of IDO activity in SF-MSCs with or without induction of the RA joint-mimicking milieu. The asterisks indicate significant differences. The graphs present the mean ± SD. h- or h+ indicate normoxic or hypoxic conditions, respectively; i- or i+ indicate the absence or presence of pro-inflammatory cytokines, respectively.

Figure 6

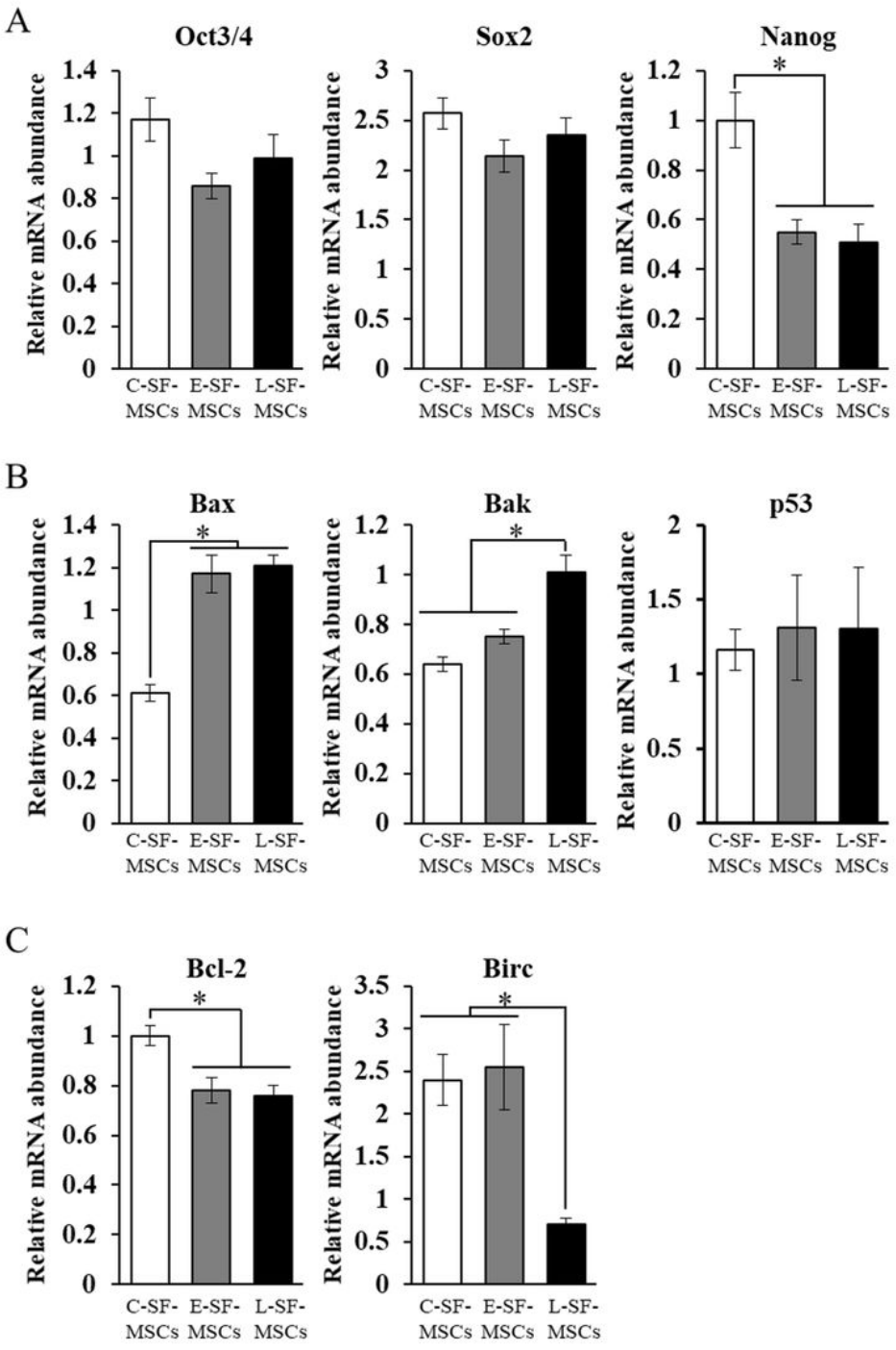

Figure 6

Analysis of gene expression level in SF-MSCs. Quantitative RT-PCR was used to evaluate (A) pluripotency, (B) pro-apoptosis, and (C) anti-apoptosis gene expression in SF-MSCs. The asterisks indicate significant differences. The graphs present mean values ± SD.

Supplementary Files

This is a list of supplementary files associated with this preprint. Click to download.

- FigureS1.tif
- TableS1HJLEE.docx
- TableS2HJLEE.docx